Archeologia e Calcolatori
22, 2011, 147-168

REMOTE SENSING APPLICATIONS IN ARCHAEOLOGY

1. Introduction

Early Remote Sensing applications in archaeology started in the 1920s, immediately after the First World War, with the use, limited at first and then increasingly common, of aerial photography for the detection of archeological sites which were partially or totally buried, or in any case not visible from the ground. This method, mostly developed in northern Europe, was systematically used till the 1970s, permitting significant discoveries. Fig. 1 shows, for instance, the Gallo-Roman *villa rustica* in Burgundy (France), discovered in 1979 thanks to aerial photography.

To achieve satisfactory results, aerial photos have to be taken with adequate photographic scale values (with respect to the dimensions of objects to be identified), in suitable periods and times – for instance, partially buried structures are more easily identifiable from on high in the early morning or late afternoons hours, thanks to shadows of relics emerging from the ground – and particular weather conditions. Fig. 2 illustrates the traces of a buried site highlighted by the comparison between two aerial photos, taken before (a) and after (b) a heavy rain.

In the 1940s the introduction of infrared films and infrared (false-color) films produced a significant shift in results, permitting even more refined evaluations, by means of traditional analog photo-interpretation techniques. There have obviously been many more traditional applications of aerial photography, aiming at producing maps related to archeological sites and their surrounding areas. The first satellite images used in archaeology were the ones known as CORONA imagery, produced by an espionage satellite operating from 1960 to 1972, equipped with two cameras, respectively forward and backward oriented, enabling it to produce stereo-photos. In that period more than 800,000 high-resolution photos were taken in the North-East area of the United States. Since 1996 – year in which they were declassified and made available to the scientific community – these photos have constituted a very interesting archive for American archaeologists (Fig. 3).

The subsequent phases in the evolution of Remote Sensing techniques in the archaeological field are related to the diffusion of sensors capable of extending data acquisition in the electromagnetic spectrum, beyond visible bands, up to the thermal infrared area (multi-spectral and hyperspectral sensors) and to the radio microwaves (radar imagery), as well as to the introduction of modern techniques for digital image processing (e.g. Parcak 2009; Lasaponara, Masini 2009; Forte, Campana, Lizza 2010).

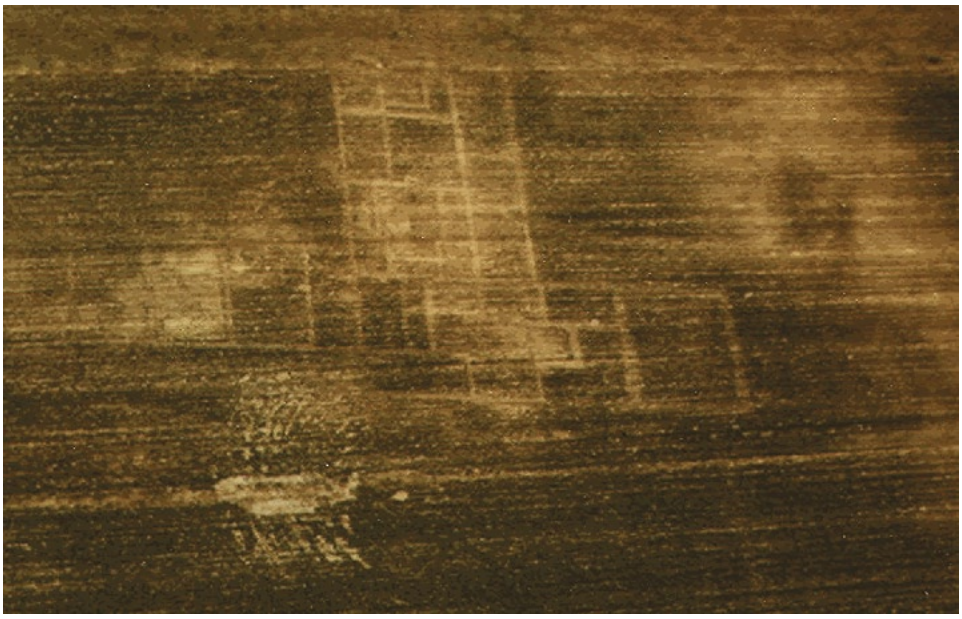

Fig. 1 – Gallo-Roman *villa rustica* in Burgundy (France) (http://www.informatics.org/france/aerial.html).

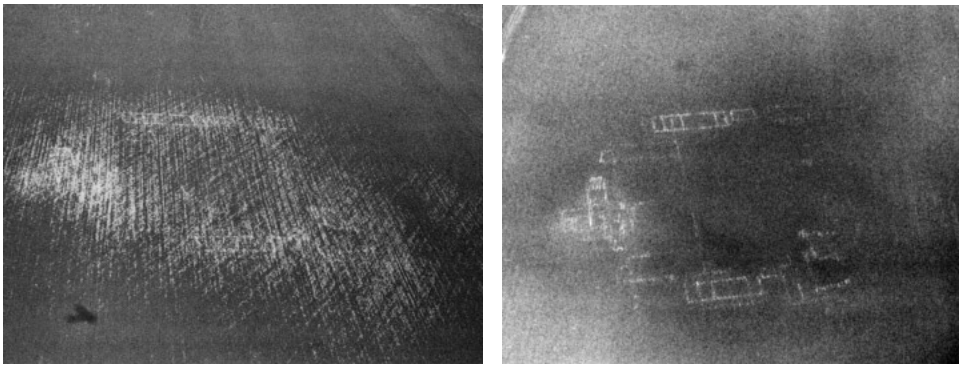

Fig. 2 – Roman villa at Grivenes (France): a) before the rain b) after the rain (Scollar *et al.* 1990).

Among the sensors used for archaeological applications, it is worth mentioning also the LiDAR (Light Detection and Ranging) and the high geometric resolution satellites, which have come into use in the last decade. The first one makes it possible to rapidly produce very dense and accurate

Fig. 3 – Ancient road network in Northern Mesopotamia (CORONA imagery) (Ur 2003).

Digital Terrain Models (DEMs), capable of satisfying the various cartographic needs; the second ones make available to archaeologists a huge amount of multi-spectral and multi-temporal data – characterized by short revisit time (even less than one week) – showing an adequate accuracy even for medium-scale maps (1:10,000, 1:5,000).

A further application of Remote Sensing is the use of thermographs from radio-controlled systems, allowing the acquisition of data related to small archaeological areas from low flying heights. Modern thermo-cameras available in the market are capable of detecting thermal gradients of some degrees centigrade and CCD sensors with which these cameras are equipped have, nowadays, very small dimensions, which in any case permit accurate thermal analyses.

Traditional Remote Sensing archaeological applications have dealt, and still deal, with the production of maps and DEMs and with the acquisition of data related to physical and environmental parameters for the detection of potential buried structures. As already said, the growing public interest

with respect to themes related to the preservation and exploitation of cultural heritage, particularly archaeological assets, has recently directed Remote Sensing applications above all towards the multi-temporal monitoring of existing archaeological sites and their surrounding areas, to study the evolution over time of the most significant environmental and anthropic parameters (change in the use of soil, characteristics of vegetation, urban sprawl, thermal anomalies, etc.). In both cases, data acquired by means of Remote Sensing techniques must be subsequently implemented into GIS which, after having modeled, analyzed and interpreted them, should enable archaeologists and public administration to provide adequate responses and decisions.

In the following subsections Remote Sensing techniques for archaeological surveys, with respect to cartographic applications and to applications for detection of buried structures, will be thoroughly outlined. Geophysical methodologies operating in contact with the earth surface (viz. Ground-penetrating Radar) have not been considered, thus limiting the study to remote operating methodologies, from airborne and satellite devices.

2. Cartographic applications

Cartographic applications are directed to the production of topographic and thematic maps of archaeological sites and their surrounding areas, to the representation of archaeological materials, to the planning of future excavation areas and of activities for the maintenance and management of an archaeological site, or as base map for the creation of GIS.

These objectives, up to a few years ago pursuable by means of traditional aerial photography, may be achieved today by means of digital images, produced by satellite or airborne sensors with high geometric resolution. These sensors are characterized, in fact, by ground sample distance (GSD) ranging from 1 m, for high resolution satellites, to 0.05 m, for airborne sensors, thus making it possible to satisfy any cartographic need ranging from 1:10,000 to 1:200 map scale.

Hyperspectral sensors are the most appropriate tools for producing thematic maps (use of the soil, extraction of road system, classification of vegetation, etc.), thanks to the image classification techniques. These maps are usually produced using supervised and unsupervised algorithms based on the assessment of spectral similarity of single pixels. Another classification technique is based upon fuzzy logic; in this case, not only spectral response, but also semantic relations between pixel groups, i.e. segments or objects, and surrounding groups, are assessed.

The raster images thus produced may be subsequently implemented into GIS environment and compared with data related to topography, geophysical features, chemical composition of soil, presence of road networks, distance

from points of water supply, etc., permitting the compilation of predictive maps of archaeological sites. This is one of the possible applications integrating Remote Sensing and GIS. The implementation of predictive models in the archaeological ambit is just based upon mutual relations among geometric entities present on the study areas.

Table 1 shows the most commonly used satellite and airborne sensors in archaeological applications, with their main features.

Sensor	Type	Airborne/Satellite	Stereo ready	minimum GSD ≅	Channels
ATM	multi-spectral	airborne	no	0.3 m	11
Ikonos II	multi-spectral	satellite	yes	1 m	4
QuickBird	multi-spectral	satellite	yes	0.7 m	4
GeoEye	multi-spectral	satellite	yes	0.7 m	4
Leica ADS40	multi-spectral	airborne	yes	0.05 m	4
Vexcel UltraCAM	multi-spectral	airborne	yes	0.018 m	4
Z/I Imaging DMC	multi-spectral	airborne	yes	0.04 m	4
AVIRIS	hyperspectral	airborne	no	4 m	224
CASI	hyperspectral	airborne	no	1 m	8
HyMap	hyperspectral	airborne	no	3 m	126
MIVIS	hyperspectral	airborne	no	3 m	102

Tab. 1 – Satellite and airborne sensors used in archaeological applications.

Fig. 4 shows the digital orthophoto of the archaeological site of Elaiussa Sebaste in Turkey, produced by a high resolution QuickBird Standard OrthoReady satellite image acquired in 2004. A GPS campaign was carried out for surveying GCPs for image georeferencing as well as for the construction of the DEM to be used for orthorectification procedures. The Elaiussa site is located on the south-eastern coast of Turkey, about 60 km from the town of Mersin. The need for an archaeological base map aimed at representing both already excavated areas and areas where further surveys and excavations were still being carried out already during the first years of excavation work (Equini Schneider 1988). Excavation campaigns conducted in the last ten years turned up many buildings, such as the temple in the south-western area, the theatre, the agorà and Byzantine basilica, the baths and the necropolis in the north-western area. Every year, newly surveyed areas are added to the already complex databases. The reciprocal positioning of findings is of primary importance for programming further excavation campaigns and directing other kinds of surveys.

Applications related to the production of DEMs may also be included in the cartographic field. Moreover, through topographic techniques (today mostly with GPS method) and already existing maps, DEMs may be obtained, in fact, also by Remote Sensing and geostatistical techniques.

DEMs obtained by means of Remote Sensing may be produced through photogrammetric techniques, from stereoscopic models, and through active

Fig. 4 – Digital orthophoto of the archaeological site of Elaiussa Sebaste (Turkey).

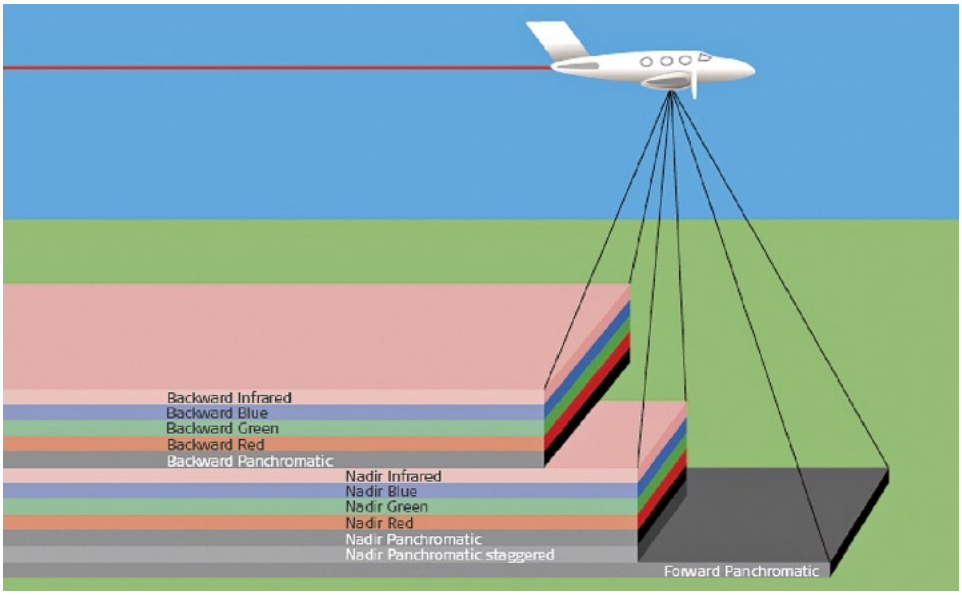

Fig. 5 – Geometry of Leica ADS40.

Fig. 6 – Survey of the site of Soknopaiou Nesos (Egypt) by captive balloon (Bitelli *et al.* 2003).

sensors (SAR, LiDAR). Both high resolution satellite sensors and modern airborne frame cameras permit the production of DEMs by digital image matching techniques, applied to stereo-pairs acquired through different modalities. Leica ADS40, in particular, is a digital aerial camera capable of acquiring simultaneously from three different points of view (forward, nadir, backward) with a 99% end lap, thus obtaining three stereo-pairs of the same area for each flight strip (Fig. 5).

Among the available active sensors, the SAR and the LiDAR are the most adequate for DEMs production. The first one is based upon the use of

Fig. 7 – Microdrone Gmbh md4-1000.

Fig. 8 – UAV (Unmanned Aerial Vehicle) Mini Helicopter System (Eisenbeiss *et al*. 2005).

Fig. 9 – Digital photorealistic model of the site of Pichango Alto (Peru) (Eisenbeiss *et al*. 2005).

interferometry techniques, while the second is based upon the measurement of the time of flight of a laser pulse transmitted by an airborne sensor.

Due to particular needs in managing archaeological sites, it is sometimes necessary to produce topographic maps on a very large scale (up to 1:20). In these cases, particular sensors may be adopted (metric, semi-metric and non-metric digital cameras, pushbroom sensors, etc.) which, placed on suitable vectors, let us to obtain metrically reliable images at very large scale. Various types of vectors may be used, from captive balloons (Fig. 6) to radio-controlled helicopters with GPS/INS system, to modern drones (Fig. 7), which dramatically reduce human intervention.

Fig. 8 shows the radio-controlled helicopter used for the 3D modeling of the archeological site of Pichango Alto in Peru (Eisenbeiss *et al.* 2005). It is a low-cost vector, equipped with a GPS/INS system and with a CCD high resolution sensor, to take vertical stereoscopic photos from an average flight height of 80 m. A very dense DEM of the archaeological site was produced through the integration between photogrammetric and terrestrial laser-scanning data (Fig. 9).

3. Detection of buried structures

Buried structures and discontinuities of the first subsoil produce a inhomogeneous distribution of humidity, namely creating preferential lines along which water accumulates, producing lineation phenomena and thermal anomalies (Dabas, Tabbagh 2000).

This anomalous distribution affects some parameters, such as the color of naked soil, the density and physical state of vegetation (Scollar *et al.* 1990), the thermal and electric capacity and conductivity. One of the objectives of Remote Sensing in archeology is the analysis of these features, represented in the form of image, to identify regular shapes referable to potential buried structures. The choice of the parameters to be analyzed is closely linked to the type of available data. In particular, the analysis of vegetation density and of soil color requires the knowledge of the spectral behavior within infrared and visible, while, with respect to thermal parameters analysis, it is necessary to know the spatial distribution of temperature. In this case, it is necessary to use images acquired by sensors capable of giving information within the thermal infrared.

3.1 *Color of soil*

The color of the soil varies with its composition and with the level of surface moisture. For the analysis of surface moisture, bands with high reflectance values are used. In the absence of vegetal covering, wet soil absorbs radiance in the near infrared, due to the opacity typical of water. At the in-

crease of wavelength, from red towards the region of reflected infrared, the contrast between dry reflecting soils and wet opaque soils tends to increase (the maximum contrast is observed at 1.40 μm ÷ 1.45 μm). On soils covered with grass, when humidity increases, the density of vegetation also increases. The reflectance value of dry soils increases when wavelength increases from blue to near infrared, while reflectance value of wet soils decreases from red to infrared with a minimum around 1.4 μm (Scollar *et al.* 1990).

The identification of an anomalous distribution of soil color is performed using the aforementioned spectral characteristics, with respect to the infrared and the red and, in particular, identifying areas characterized by sudden drops of reflectance. This may be obtained by the following map algebra elaboration:

$$G_s = abs\frac{[R(x+1,y)-R(x,y)]}{R(x,y)} + abs\frac{[(R(x,y+1)-R(x,y)]}{R(x,y)} + abs\frac{[NIR(x+1,y)-NIR(x,y)]}{NIR(x,y)} + \frac{[NIR(x,y+1)-NIR(x,y)]}{NIR(x,y)} \quad \textit{(Eq. 1)}$$

where:
– G_s is the soil color index;
– R is the *DN (Digital Number)* of red channel;
– *NIR* is the *DN* of near infrared channel.

This methodology offers its best results on recently ploughed soils and it requires, in any case, a soil not covered by vegetation.

3.2 *Influence upon vegetation*

The density and physical state of vegetation give information on the permeability and thickness of the vegetal layer of soil. Therefore, higher density and better physical state of vegetation are observed in thicker vegetal soils, while reduced and anomalous growth is observed with the presence of buried structures reducing the thickness of vegetal soil. The study of vegetation as an indicator of potential buried structures relies on the spectral response in the visible and in the near infrared wavelengths, as well as on the heat emission in the thermal infrared.

Vegetation reflects about 4% in the blue region, 15% in the green, 6% in the red and it is highly reflective in the near infrared. Vegetation as an environmental indicator is analyzed with respect to the density of the foliar system and to the physical state. These features are observed through the behavior of reflectance and of emission of the first layer of vegetated surface. During the heating phase, healthy vegetation, not subject to water stress, shows a lower amount of temperature than the one of inert surface for complex thermo-stability systems. Anomalous growth, due to the potential presence of buried structures and the subsequent reduction of vegetated soil, appears in the following radio-metric anomalies:

– drop of reflectance in near infrared;

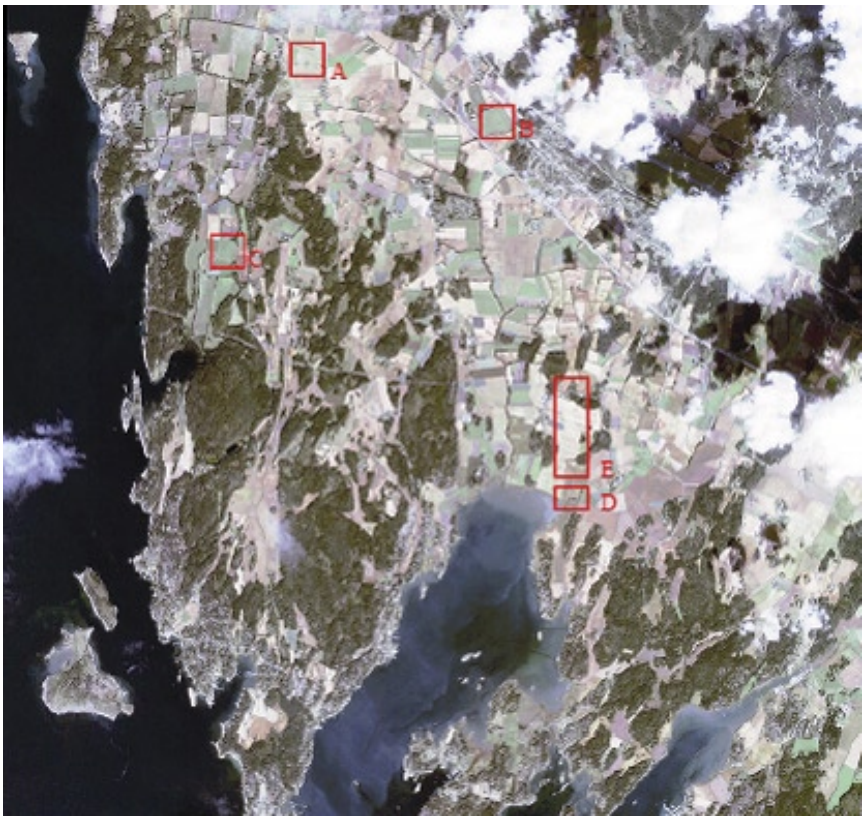

Fig. 10 – Localization of the areas characterized by anomalies.

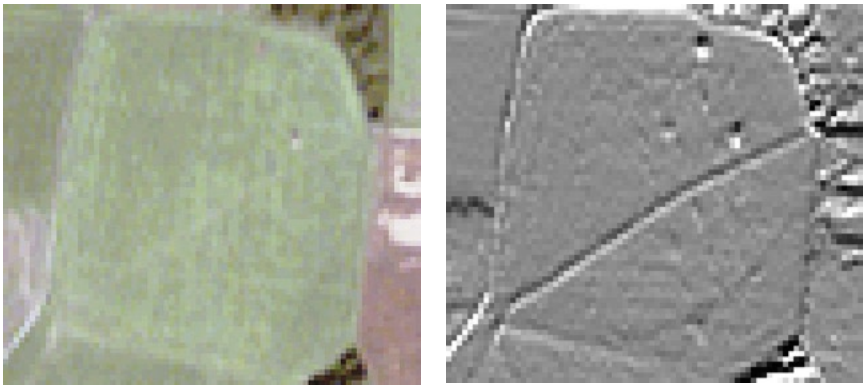

Fig. 11 – Comparison between true color (a) and S index (b) images for C area.

– increase of reflectance in red;
– closer dependence of leaves temperature on the external temperature.

These alterations may be identified through:

$$S = h + k \cdot \arctan \frac{I_{NIR}}{B + R + I_{RV} + I_{RT}} \qquad \textit{(Eq. 2)}$$

where:
– S is the physical state of vegetation;
– k are constants for image enhancement (*arctan* function is used to limit high values);
– I_{NIR} is the intensity of reflected radiance around 0.8μm (near infrared);
– B is the intensity of reflected radiance around 0.45 μm (blue);
– R is the intensity of reflected radiance around 0.7 μm (red);
– I_{RV} is the intensity of reflected radiance around 1.55 μm (red);
– I_{RT} is the intensity of emitted radiance in 9÷12 μm (thermal infrared).

An application related to the analysis of the above-mentioned parameters was carried out upon an Ikonos image (Fig. 10) in an area around Rygge in Norway (Grøn *et al.* 2006). Experimentation made it possible to produce an image within which the DNs represent the corresponding values of the *S* index, and to identify some areas characterized by anomalies referable to potential buried structures (Fig. 11).

The analysis of the anomalous humidity distribution, therefore of vegetation, may also be performed using radar data (SAR, InSar). The advantage of radar sensors is that they can be used independently from weather conditions (Lillesand, Kiefer 2000); in arid environments, moreover, the radar impulse is capable of penetrating up to 2 m below soil surface, thus enabling us to identify buried structures. The Paleolithic and Neolithic remains in the eastern part of the Sahara desert have been identified, for instance, through radar techniques (McCauley *et al.* 1982).

A significant application of the use of SAR data has been carried out on the island of San Clemente in the Channel Islands, off the southern California coast, both for the analysis of vegetation and for the assessment of dielectric and thermal properties of the soil (Comer, Blom 2007). Other applications reveal, for instance, the importance and the potential of this technology applied to archaeology, both for the production of DEMs and for the detection of buried archaeological sites.

3.3 *Thermal parameters*

The first subsoil water, accumulated in preferential lines produced by buried structures, rises to the surface thanks to capillarity and it subtracts heat form the soil, leaving as a trace a drop in soil temperature and affecting

some physical features such as thermal capacity, thermal inertia and thermal conductivity. The distribution of temperature, capacity and thermal conductivity are essential aspects in the field of archaeological research.

The assessment of soil humidity, therefore of its anomalous distribution, is performed through thermal capacity, thermal inertia, thermal conductivity and through the trend of surface thermal gradients.

3.3.1 Thermal capacity and thermal inertia

Thermal capacity is the expression of specific heat and of the mass underlying the observed surface. The most humid zones are characterized by higher amounts of inertia and thermal capacity. There are two procedures related to the heating or cooling phases in two different instants t_1, t_2.

In the first case:

$$I = \frac{Q}{\Delta T} \qquad \textit{(Eq. 3)}$$

where:

– I is thermal inertia;
– Q is the absorbed heat in the interval t_1, t_2;
– ΔT is the variation of temperature related to the mass represented by a generic pixel in the interval t_1, t_2.

The incident energy coming from the sun is partly reflected, partly absorbed and partly transmitted. This behavior, expressed by the Kirchhoff's law, lets to calculate Q as a complement of the reflected energy. As a matter of fact, supposing energy transmission phenomena are absent and heat by irradiation keeps constant in the t_1-t_2 interval, Q is given by the following:

$$Q = E_a \qquad \textit{(Eq. 4)}$$

where E_a is the absorbed energy.

For the principle of energy conservation:

$$\rho + \tau + \alpha = 1 \qquad \textit{(Eq. 5)}$$

where:

$\rho = \frac{E_r}{E_{inc}}$ is the percentage of reflected energy;

$\tau = \frac{E_t}{E_{inc}}$ is the percentage of transmitted energy;

$\alpha = \frac{E_a}{E_{inc}}$ is the percentage of absorbed energy.

For an opaque body, $\tau = 0$, therefore Eq. 4 becomes:

$$Q = E_a = \frac{R_a}{\rho(\lambda)}(1 - \rho(\lambda)) \qquad \textit{(Eq. 6)}$$

where:
– $R_a(\lambda)$ is the radiance reflected by the sensor;
– $\rho(\lambda)$ is reflectance.

In the second case the thermal capacity may be calculated by:

$$C_m = \frac{A_0}{\ln \frac{T_{t1} - T_{t3}}{T_{t2} - T_{t3}}} \qquad \textit{(Eq. 7)}$$

where:
– A_0 is a constant;
– T_{t1}, T_{t2}, T_{t3} are the temperature, respectively, at the initial, intermediate and final instant, on the cooling phase.

With respect to thermal gradients on the surface, with a single available thermograph image, the trend of humidity may be identified observing that:
– humid areas are characterized by negative thermal anomalies regarding to the surrounding area;
– humid areas have high values of conductivity, therefore limited thermal gradients.

On the basis of these considerations the product between temperature $T(x, y)$ and absolute gradient $G(x, y)$ can be calculated by the following:

$$G = abs[T(x+1, y) - T(x, y)] + abs[T(x, y) - T(x, y+1)] \qquad \textit{(Eq. 8)}$$

$$m(x, y) = T(x, y) \cdot G(x, y) \qquad \textit{(Eq. 9)}$$

The most humid areas are characterized by lower $m(x,y)$ amounts represented by pixels with low DNs.

3.3.2 Thermal conductivity

The assessment of thermal conductivity as an index of potential buried structures is performed in a qualitative way, starting from the consideration that water is a good heat conductor, therefore to more humid zones correspond low temperature gradients.

Let's observe the behavior of a generic pixel during the heating phase. Supposing among various pixels there is no possibility to transmit heat and therefore, as a direct consequence, pixels corresponding to objects which

absorb higher heat quantity are characterized by temperature increments proportional to the quantity of absorbed heat. In reality, this proportionality decreases with the increase of the thermal conductivity of every single pixel.

Relating the spatial distribution of absorbed heat by every single pixel with the corresponding distribution of temperature increments, a qualitative index of thermal conductivity may be evaluated. Namely, this index can be obtained through:

$$\mathrm{Ict}(x, y) = \mathrm{abs}[\mathrm{scQ}(x, y) - \mathrm{sc}\Delta\mathrm{T}(x, y)] \qquad \textit{(Eq. 10)}$$

with:

$$\mathrm{scQ}(x, y) = abs[Q(x+1, y) - Q(x, y)] + abs[Q(x-1, y) - Q(x, y)] + \\ + abs[Q(x, y+1) - Q(x, y)] + abs[Q(x, y-1) - Q(x, y)] \qquad \textit{(Eq. 11)}$$

$$\mathrm{sc}\Delta\mathrm{T}(x, y) = abs[\Delta\mathrm{T}(x+1, y) - \Delta\mathrm{T}(x, y)] + abs[\Delta\mathrm{T}(x-1, y) - \Delta\mathrm{T}(x, y)] + \\ + abs[\Delta\mathrm{T}(x, y+1) - \Delta\mathrm{T}(x, y)] + abs[\Delta\mathrm{T}(x, y-1) - \Delta\mathrm{T}(x, y)] \qquad \textit{(Eq. 12)}$$

where:

– Q is the quantity of absorbed heat in the point x, y;
– $\Delta T(x, y)$ is the variation of temperature in the pixel with coordinates (x, y) due to the absorbed heat.

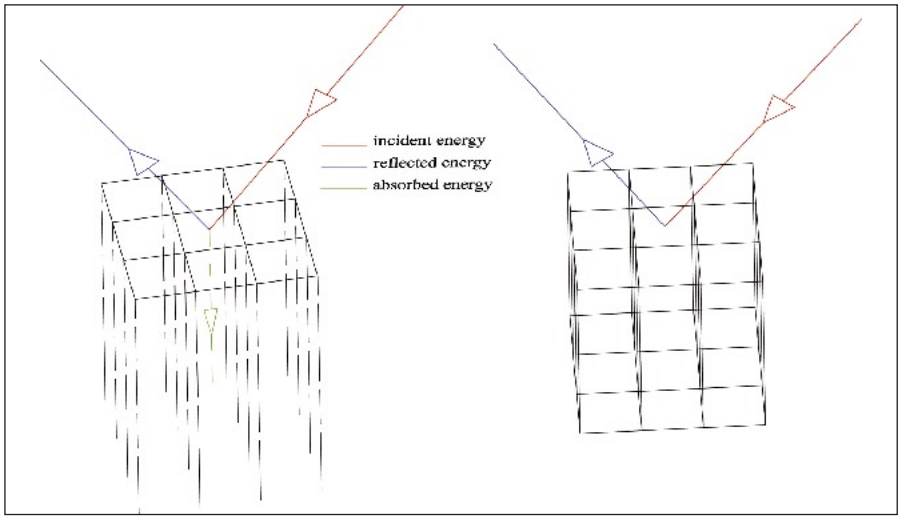

Fig. 12 – Energy absorbed and reflected by a single prism.

Suppose two thermographs relative to subsequent instants are available; the first is related, for instance, to a morning acquisition, the second one to an acquisition made some hours later (heating phase). Every pixel of both images may be considered as the upper face of an undetermined prism: the four lateral surfaces of the prism touch the respective surfaces of prisms related to adjacent pixels (Fig. 12).

During the heating phase the heat absorbed by any single prism spreads through its lateral faces more or less rapidly, in relation to the thermal conductivity. If conductivity is zero and the external surface is subject to a gradient of the absorbed heat quantity (coalbedo: complement of reflected energy), heat does not flow through lateral surfaces and the temperature gradient among adjacent pixels increases proportionally to the energy absorbed by outside.

This particular pattern of behaviour, related to a unreal condition (total absence of thermal conductivity), implies that at the increase of intensity of absorbed energy the ratio between the radiance gradient *G* and the radiance *N* keeps constant in time, according to the following:

$$G = abs[N(x+1,y) - N(x,y)] + [N(x,y) - N(x,y+1)] \qquad \textit{(Eq. 13)}$$

$$G = \frac{abs[N(x+1,y) - N(x,y)]}{N(x,y)} + \frac{abs[N(x,y) - N(x,y+1)]}{N(x,y)} \qquad \textit{(Eq. 14)}$$

This latter relation indicates the normalized gradient and shows that in the reflected radiance domain, at varying the intensity of the luminous source, variation of normalized gradient remains zero. Supposing two subsequent acquisitions at t_1 and t_2 instants:

$$G = abs[N(x+1,y) - N(x,y)] + [N(x,y) - N(x,y+1)] \qquad \textit{(Eq. 15)}$$

In the case of thermograph images *N(x, y)* amounts are substituted by temperature values *T(x, y)* and the Eq. 15 becomes:

$$G = \frac{abs[N(x+1,y) - N(x,y)]}{N(x,y)} + \frac{abs[N(x,y) - N(x,y+1)]}{N(x,y)} \qquad \textit{(Eq. 16)}$$

This relation is equal to zero in the absence of conductivity and it shows amounts greater than zero in other cases. In archaeological applications this process makes it possible to identify geometrically regular areas, characterized by high thermal conductivity amounts.

The analysis of thermal parameters requires the knowledge of the spatial distribution of temperature as well as an accurate choice of the kind of datum to use. The following application is an example of this procedure.

The study area was related to the archaeological sites of the Roman Villa del Casale and Sofiana, in the province of Enna, in Italy (Fig. 13). Images were acquired by the hyperspectral MIVIS sensor in June 2002, during an aerial photographic mission aimed at performing archaeological surveys. Two flights were carried out with respect to each archaeological site, at different times; the first one at 9.30, the second one at 12.30, so that radiometric variations caused by soil heating could be identified, from the comparison between the two images. Each flight consists of two strips having flying heights of 1,500 m; the images are characterized by GSD of 3 m.

The above-mentioned techniques were applied to acquired images, aimed at producing two images related, respectively, to inertia and to thermal conductivity (Emmolo *et al.* 2004). Fig. 14 shows the comparison among true color (a), thermal inertial (b) and thermal conductivity (c) images for C area; it is possible to notice some anomalies referable to potential buried structures. The inverse tangent function was then applied to these images. This function tends to two horizontal asymptotes, therefore it smoothes the variability when thermal inertia amounts are high, in this way enhancing the image contrast.

Fig. 13 – Localization of the archaeological sites of the Villa del Casale (A) and Sofiana (B).

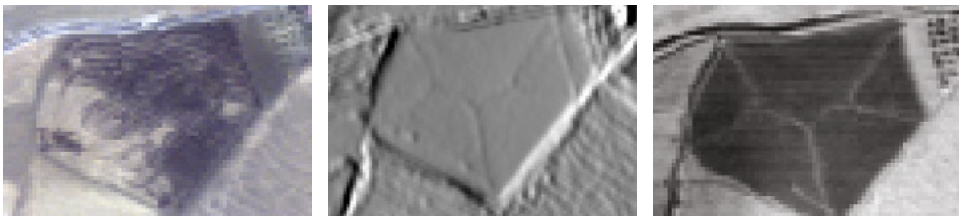

Fig. 14 – Comparison among true color (a), thermal inertial (b) and thermal conductivity (c) images for C area.

3.4 *Principal Components Analysis*

The Principal Components Analysis (PCA) is a traditional technique of data simplification used in multivariate statistics. The first objective of this method is the reduction of a very high number of variables (representing as many features of the analyzed phenomenon) to some latent variables. PCA, from the mathematical point of view, consists of a 3D conformal coordinate transformation decorrelating multivariate data through the roto-translation axes of the original spatial system in such a way as to represent this space without correlation, in a spatial system with new components (Richards, Jia 1986). Considering the remotely sensed images as numerical matrixes, PCA can be successfully applied also in the field of image processing, as hyperspectral Remote Sensing technique. In fact, in hyperspectral sensors the operation of reducing the number of significant bands without a substantial loss of information is a remarkable facility for researchers.

PCA enables us to minimize a problem typically encountered in hyperspectral data processing: high correlation among various bands, which causes information redundancy, therefore noise, reducing the capability of discriminating among pixels with similar reflectance values. These components enhance similarities and differences, detected and processed by the algorithm among corresponding pixels of starting hyperspectral images. The incidence of correlation is particularly high for vegetated surfaces. A negative correlation between near infrared and red is in fact observed, as well as a positive correlation among visible bands. This phenomenon is due to the spectral characteristics of vegetation, which has a high reflectance value in the near infrared; it has, vice versa, low reflection values in the red channel.

Since in some cases vegetation constitutes an important mediation factor for the detection of buried structures, PCA is successfully used also in the archaeological field, not only for vegetated surfaces, but also on naked soils; in this case the different spectral behavior of red and of the near infrared in presence of humidity comes into play. PCA creates new images decorrelated among them, called principal components, equal to the number

Fig. 15 – Linear anomaly detected in the area surrounding Sofiana.

of channels processed through the roto-translation of the coordinate system in which each point may be positioned in relation to the amounts of each channel. The first component (PC1) is the result of the sum of all the bands, each with a weight proportional to the level of originality of information it contains. The second (PC2) represents the absolute value of the discrepancy in terms of reflectance of every pixel with respect to the PC1 values. The following components contain a decreasing percentage of information and an increasing percentage of noise. The first two components already give a significant contribution for revealing traces and discontinuity of archaeological interest.

For instance, observing the MIVIS image related to the Villa del Casale, acquired at 9.30, it is possible to perform this type of analysis both on the 93 bands related to the part of the reflection spectrum and on the 10 thermal infrared bands. In the first case, the RGB color combination of the first three principal components makes photo-interpretation operations particularly easy; moreover, the application upon the first principal component of image enhancement techniques, such as for instance, the Gaussian high pass filter, makes it possible to identify the anomalies already detected in the previous paragraph. In the second case the application of this type of analysis of thermal infrared bands enabled us to concentrate useful information in one single band (PC1) and to increase the contrast among the areas subjected to thermal anomalies and the surrounding areas. Fig. 15 shows the results of the above-described process.

4. Conclusion

The above-mentioned applications show that Remote Sensing is a valuable aid in archaeological surveys. In particular, aerial photography and multi-spectral satellite data are very suitable for cartographic applications, and makes it possible to acquire very quickly various kinds of information concerning landscape, morphology, and vegetation, and to produce thematic maps. These maps, especially if implemented into GIS, are of great utility for the archeologist.

As a matter of fact, remotely-sensed data are often disaggregated, not georeferenced and characterized by format, scale and uncertainty amounts which differ greatly from each other, and therefore are difficult to compare and interpret. In order to obtain an appropriate and widespread use and management of these data, therefore, it is necessary to resort to GIS (Star *et al.* 2010). These two techniques are fully complementary with each other for archaeological surveys. Each of them offers a very important, yet partial contribution; only the combined use of both allows the full exploitation of their potential for an in-depth understanding and an effective utilization of data related to an archaeological site.

Pietro Orlando, Benedetto Villa
DICA – Department of Civil, Environmental and Aerospace Engineering
University of Palermo (Italy)

REFERENCES

Bitelli G., Girelli V.A., Tini M.A., Vittuari L. 2004, *Low-height aerial imagery and digital photogrammetrical processing for archaeological mapping*, «International Archives of Photogrammetry, Remote Sensing and Spatial Information Sciences», 35, B5, 498-503.

Campbell J.B. 2006, *Introduction to Remote Sensing*, London, 4th ed., Taylor & Francis.

Comer D., Blom R. 2007, *Detection and identification of archaeological sites and features using Synthetic Aperture Radar (SAR) data collected from airborne platform*, in J. Wiseman, F. El-Baz (eds.), *Remote Sensing in Archaeology*, New York, Springer, 103-109.

Dabas M., Tabbagh A. 2000, *Thermal Prospecting*, *Archaeological Method and Theory: An Encyclopedia*, New York, Garland Publishing, 626-638.

Eisenbeiss H. 2006, *Applications of photogrammetric processing using an autonomous model helicopter*, «International Society for Photogrammetric and Remote Sensing», 36, 1, T08-35.

Eisenbeiss H., Lambers K., Sauerbier M., Zhang L. 2005, *Photogrammetric documentation of an archaeological site (Palpa, Peru) using an autonomous model helicopter*, «International Archives of Photogrammetry, Remote Sensing and Spatial Information Sciences», 34, 5/C34, 238-243.

Emmolo D., Franco V., Lo Brutto M., Orlando P., Villa B. 2004, *Hyperspectral techniques and GIS for archaeological investigation*, «International Archives of Photogrammetry, Remote Sensing and Spatial Information Sciences», 35, B7, 492-497.

Equini Schneider E. 1988, *Elaiussa Sebaste I*, Roma, L'Erma di Bretshneider.

Forte M., Campana S., Lizza C. (eds.) 2010, *Space, Time, Place. Third International Conference on Remote Sensing in Archaeology (Tiruchirappalli, Tamil Nadu, India 2009)*, BAR International Series 2118, Oxford, Archaeopress.

Grøn O., Christensen F., Orlando P., Baarstad I., Macphail R. 2006, *Hyperspectral and multispectral perspectives on the prehistoric cultural landscape; the ground-truthed chemical character of prehistoric settlement and infrastructure as identified from space*, in S. Campana, M. Forte (eds.), *From Space to Place. Proceedings of the 2nd International Conference on Remote Sensing in Archaeology (Rome 2006)*, BAR International Series 1568, Oxford, Archaeopress, 143-147.

Kelong T., Yuqing W., Lin Y., Riping Z., Wei C., Yaobao M. 2008, *A new archaeological Remote Sensing technology*, «International Archives of Photogrammetry, Remote Sensing and Spatial Information Sciences», 37, B7, 221-224.

Lasaponara R., Masini N. 2009, *Remote Sensing for Cultural Heritage Management and Documentation*, «Journal of Cultural Heritage», 10S, e1-e2, Paris, Elsevier.

Lee D., Farr T.G. 2007, *The use of Interferometric Synthetic Aperture RADAR (InSar). Archaeological investigation and cultural heritage preservation*, in J. Wiseman, F. El-Baz (eds.), *Remote Sensing in Archaeology*, New York, Springer, 89-94.

Lillesand T.M., Kiefer R.W. 2000, *Remote Sensing and Image Interpretation*, New York 3rd ed., John Wiley & Sons.

McCauley J.F., Schaber G.G., Breed C.S., Grolier M.J., Haynes C.V., Issawi B., Elachi C., Blom R. 1982, *Subsurface valley and geo-archaeology of eastern Sahara by shuttle radar*, «Science», 218, 1004-1020.

Mueller J.W. 1974, *The use of sampling in archaeological survey*, «Memoir of the Society for American Archaeology», 28, 28-36.

Parcak S.H. 2009, *Satellite Remote Sensing for Archaeology*, London, Routledge.

Richards J.A., Jia X. 1986, *Remote Sensing Digital Image Analysis: An Introduction*, Berlin, Springer.

Scollar I., Tabbagh A., Hesse A., Herzog I. 1990, *Archaeological Prospection and Remote Sensing*, New York, Cambridge University Press.

Shennan I., Donoghue D.N.M. 1992, *Remote Sensing in archaeological research*, «Proceedings of the British Academy», 77, 223-232.

Star J.L., Estes J.E., McGwire K.C. (eds.) 2010, *Integration of Geographic Information Systems and Remote Sensing*, Cambridge, Cambridge University Press.

Syed A., Drummond J., Hanson S. 2008, *Discovering archaeological cropmarks: A hyperspectral approach*, «International Archives of Photogrammetry, Remote Sensing and Spatial Information Sciences», 37, B7, 361-366.

Tan K.L., Wan Y., Zhou X., Song D., Duan Q. 2006, *Application of Remote Sensing technology in the archaeological study*, «International Journal of Remote Sensing», 27, 3347-3363.

Tan K.L., Wan Y.Q., Yang Y.D. 2005, *Archaeological exploration research of hyperspectral Remote Sensing*, «Journal of Infrared and Millimeter Waves», 24, 437-442.

Ur J. 2003, *CORONA satellite photography and ancient road networks: A Northern Mesopotamian case study*, «Antiquity», 77, 102-105.

Wilson D.R. 2000, *Air Photo Interpretation for Archaeologists*, Stroud, Tempus.

Winterbottom S.J., Dawson T. 2005, *Airborne multi-spectral prospection for buried archaeology in mobile sand dominated systems*, «Archaeological Prospection», 12, 205-219.

ABSTRACT

In recent years Remote Sensing applications in archaeology have become increasingly frequent. This plurality of applications depends mostly on the rising interest of the scientific

community in modern methods for surveying geographic data, which have become increasingly powerful, automatic and reliable. Remote Sensing, with its various techniques, offers the rapid acquisition of a huge quantity of metric and qualitative data in order to describe or to identify archaeological sites. For an appropriate and widespread use of these data, it is still necessary to have recourse to GIS techniques; as a matter of fact, only the combined use of both methodologies provides a full exploitation of their potential for an in-depth understanding and an effective utilization of data related to an archaeological site. The authors illustrate some case studies concerning use of remote sensed data for cartographic applications and detection of possible buried archaeological structures.